

Molecular Simulation of Polyelectrolyte Conformational Dynamics under an AC Electric Field

Hongjun Liu, Yingxi Zhu,* and Edward Maginn*

Department of Chemical and Biomolecular Engineering, University of Notre Dame, Notre Dame, Indiana 46556

Received February 18, 2010; Revised Manuscript Received April 7, 2010

ABSTRACT: We use a coarse-grained molecular dynamics method to study the behavior of a flexible polyelectrolyte (PE) chain in an explicit salt solution with varied valence under an ac electric field. Simulations in the absence of electric field and under dc electric field are used to determine the critical field strength and intrinsic chain relaxation frequency. Our results show that the PE chain breathes with applied ac frequency and becomes dynamically stretched, only when the applied field strength exceeds the critical field strength and the applied ac frequency is comparable to or less than the intrinsic relaxation frequency of the PE chain.

I. Introduction

Polyelectrolytes (PEs) are polymers that contain charge groups along their backbone or side groups, including many biopolymers such as DNA, RNA, and proteins. They possess broad applications from energy to medical diagnosis. Electrophoresis is widely used to separate PEs.^{1,2} A molecular understanding of the complex behavior of PEs in an applied electric field will greatly advance current electrophoretic applications. Analytical theory can well describe the free-draining behavior for longer chains, yet fails to explain a nonmonotonic behavior for oligomers.³ Computer simulation provides insight to bridge this gap. Two recent publications using mesoscopic simulations have investigated the transition from oligomers to long chains in detail,^{4,5} in which the importance of hydrodynamic interactions (HI) in PE electrophoresis is emphasized. Without HI, the mobility of PE decreases with chain length and saturates at a constant value for long chains. In contrast, simulation with HI can accurately reproduce the experimentally observed nonmonotonic behavior of mobility, whereby mobility increases for oligomers, reaches a maximum for intermediate chain lengths, and slowly decreases toward a plateau for long chains.

The hydrodynamic screening length depends on the ion concentration in the vicinity of a PE chain. The more salt is added to the system, the higher is the ion density around the chain and the shorter length scale is the HI. On a length scale comparable to the Debye length, cooperative dynamics in PE chain segments become decoupled. For instance, the effective friction per monomer in a long PE chain becomes independent of chain length.^{6–8} When screening eliminates the need to explicitly account for HI, the implicit fluid method (Langevin dynamics) provides a good physical description of PEs in electric fields. Langevin dynamics has been extensively applied to study PEs in salt-free solution,⁹ in monovalent salt,^{10–12} and in multivalent salt^{13–15} as well as in electric fields.^{16–21} Netz demonstrated that a collapsed PE can be unfolded when the electric field strength is stronger than a critical value.^{19,20} The critical field strength exhibits a power-law dependence on chain length with a negative exponent. Therefore, in an electrophoresis experiment, long chains are expected to be unfolded and separate out earlier than short chains when the applied electric field strength slowly increases. The static and

dynamic properties of the PE remain unaffected below the critical field strength. Hsiao also suggested a similar scaling for PEs in multivalent salt solutions and showed that the scaling exponent depends sensitively on the salt valence.^{16,17}

Recently, there is an increasing interest in using ac electric fields to manipulate biopolymers in solution.^{22–27} Dielectrophoresis under an ac field instead of a dc field has been explored to avoid ionic screening, electrochemical reactions, and other undesirable electrokinetic effects. Several theories have suggested that ac polarization of PEs is largely due to motions of counterions, including condensed counterions and diffuse counterions. The polarizability and radius of gyration of PE chains are maximized along the field direction.²⁸ Walti et al. suggested that the major contribution to chain stretching is from the ac-field-induced torque, supplemented by a small bias force provided by ac-field-induced flow.²⁹ However, Cohen pointed out that a sufficiently strong ac field can cause the polymer to extend spontaneously to almost its full contour length without a bias.³⁰ Kaji et al. have experimentally found that low-frequency ac electric fields induce a drastic conformational change in double-stranded long DNA, from a random-coiled conformation to a stretched conformation in polymer solution,^{31,32} and in an agarose gel.^{33,34} Although an empirical range of ac frequencies and a mechanism behind chain stretching have been suggested, an understanding of the underlying physics remain far from complete, and a detailed molecular picture is highly needed.

In this article, we study the structural dynamics of a single linear PE in different valence salt solutions under an applied ac electric field. To examine ac-field-induced PE chain stretching, we use a collapsed PE chain in a multivalent solution as a model system. Our results show that a nonequilibrium unfolding transition occurs at sufficiently high ac field strength and sufficiently low frequency. To our best knowledge, it is the first molecular simulation of a PE system in an ac electric field. The rest of the paper is organized as follows. In the next section we introduce the employed simulation model. In section III, the main results of this study are presented and discussed. We give our final remarks in section IV.

II. Model and Simulation Method

We employ Langevin dynamics simulations using the LAMMPS package³⁵ to study the behavior of linear flexible PEs of different

*To whom correspondence should be addressed. E-mail: yzhu3@nd.edu (Y.Z.); ed@nd.edu (E.M.).

chain lengths. Our model system consists of a single PE chain and explicit counterions and salt. The PE is modeled by a flexible bead–spring chain with N monomers. The adjacent monomers are connected to each other by finitely extensible nonlinear elastic (FENE) bonds

$$U_{\text{FENE}}(r) = -\frac{1}{2}kb_{\text{max}}^2 \ln\left(1 - \frac{r^2}{b_{\text{max}}^2}\right) \quad (1)$$

where the stiffness parameter is $k = 7\epsilon$ and the maximum extension is $b_{\text{max}} = 2\sigma$.¹⁴ Our set of FENE parameters belongs to the semiflexible category. The average bond length is 1.1 in the absence of electric field and at weak field strengths. At strong field strengths, the bond length is extended under dc field and oscillates at a range of 1.09 σ and 1.18 σ under ac field. Each monomer with a mass m and a diameter σ carries a negative charge $-e$. N counterions each with a charge $+e$ are used to neutralize the system. Additional salt is added to system to collapse the PE chain. All ions are modeled by charged spheres with the same mass m and diameter σ . A purely repulsive Lennard-Jones potential of the Weeks–Chandler–Andersen (WCA) form³⁶

$$U_{\text{WCA}}(r) = \begin{cases} 4\epsilon[(\sigma/r)^{12} - (\sigma/r)^6] + \epsilon & r \leq 2^{1/6}\sigma \\ 0 & r > 2^{1/6}\sigma \end{cases} \quad (2)$$

is used for excluded volume interactions between all particles (including monomers and ions), where ϵ is the energy well depth and σ is the diameter of the spheres. Here ϵ and σ define the energy and length scale of simulations. All observables are expressed in reduced units. The solvent is treated as a uniform dielectric medium with a dielectric constant ϵ_r . The electrostatic interactions between charged particles

$$U_{\text{Coul}}(r) = \frac{q_i q_j / \epsilon_r k_B T}{r} \quad (3)$$

are calculated with particle–particle particle–mesh (P^3M) solver. The Bjerrum length $l_B = e^2 / 4\pi\epsilon_0\epsilon_r k_B T$ is set to 2.5 σ .

The simulations are carried out under periodic boundary condition in a rectangular parallelepiped box. The dimension of the box is varied to reach a constant monomer concentration $c_{\text{PE}} = 0.0001$ according to $1.6N \times 79.06 \times 79.06$. The added salt concentration is set to be the equivalence point. The salt concentration is $c_s = c_{\text{PE}}/q_s$, where q_s is the valence of the salt. It has been shown that the chain obtains the most compact structure at this salt concentration in the absence of an electric field. We use the Langevin equation of motion with dissipative and random forces in addition to the conservative force. Dissipative and random forces implicitly model the solvent effect and are coupled to satisfy the fluctuation dissipation theorem. We ignore the hydrodynamics interaction at this stage. Electric force $F_E = q_i E$ comes into the equation of motion as a conservative force. Langevin dynamics simulations with a damping constant of 0.4 are carried out with integration time step 0.01. After an equilibration time of 10^6 steps, 10^7 steps are used to accumulate data for analysis. The ac electric field feature is an in-house extension to the standard LAMMPS package. The applied electric field in our study is well beyond the linear response regime in order to observe the conformational transition. For the PSS (polystyrenesulfonate) system with 2.5 Å between charges, a reduced electric field of $E = 0.1$ translates to an experimental field of $E_{\text{exp}} \sim 5 \times 10^6$ V/m, while a reduced frequency of $f = 1/7000$ corresponds to an experimental frequency of $f_{\text{exp}} \sim 143$ MHz.

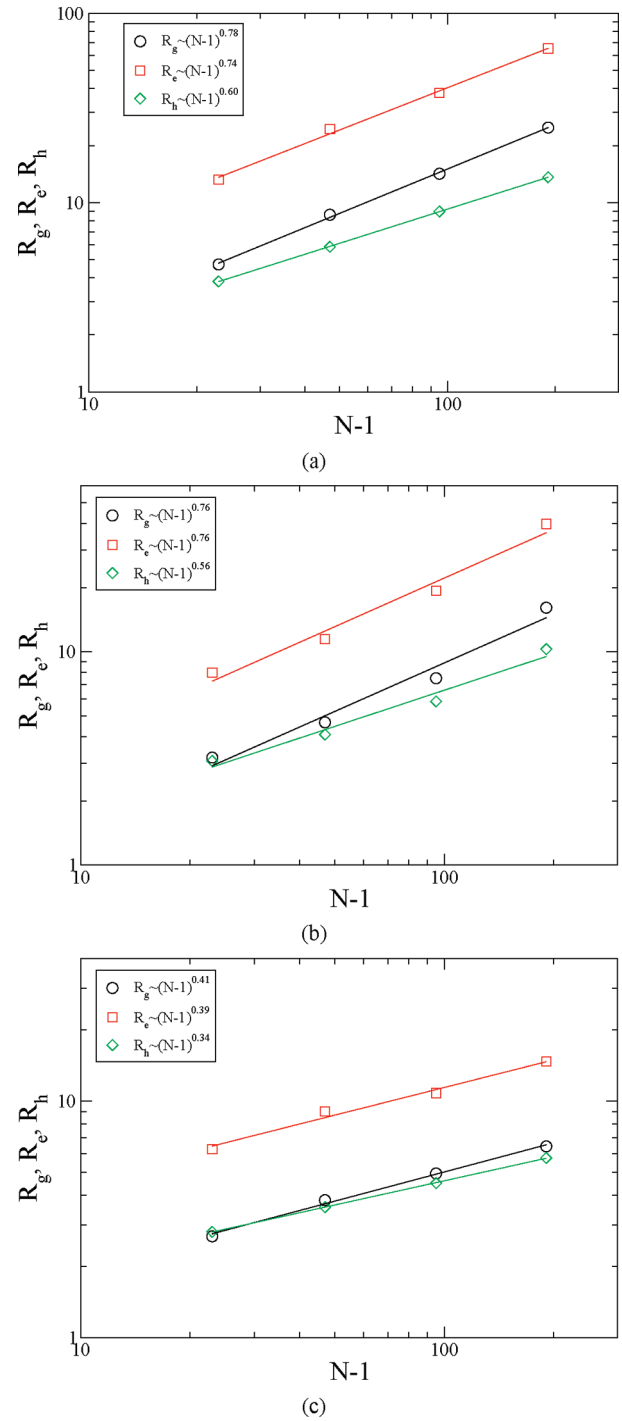


Figure 1. Scaling of the radius of gyration R_g , the end-to-end distance R_e , and the hydrodynamic radius R_h for the PE chain at an equivalent concentration of salt solutions without the electric field added with (a) monovalent salt, (b) divalent salt, and (c) trivalent salt.

III. Results and Discussion

In the next two subsections, the results of benchmark calculations are reported for a PE in the absence of an electric field and under an external dc electric field, respectively. Following this, results are presented for the conformational dynamics of the PE system in the presence of an ac electric field.

Chain Scaling and Relaxation. The PE chain conformation can be characterized by the average end-to-end distance R_e^2 , the radius of gyration R_g^2 , and the hydrodynamic radius R_h , where $1/R_h = (1/N) \sum_{i \neq j} \langle 1/|\vec{r}_i - \vec{r}_j| \rangle$. All three quantities are

expected to exhibit a power law scaling, $R \sim (N-1)^\nu$, where the scaling exponent ν depends on the system. For a neutral polymer with a self-avoiding walk behavior, $\nu = 0.588$, while for a fully charged PE without electrostatic screening (no counterions and no salt), $\nu = 1^9$ and $\nu = 0.74^{10}$ reported for the salt-free solution. Adding salt to a PE solution screens the electrostatic interactions between the PE monomers on the Debye length scale and thus reduces the scaling exponent. Hsiao studied the tetravalent salt concentration dependence of the swelling exponent ν and found that ν shows a V-shaped curve, that is, ν decreases and then increases with increasing salt concentration. A minimum ($\nu \sim 0.34$) smaller than the self-avoiding walk value occurs near the equivalent concentration.¹⁴ Figure 1a–c shows the scaling for a PE chain in the absence of an electric field and in the presence of the equivalent monovalent, divalent, and trivalent counterions, respectively. For all three salts, R_e and R_g give similar effective scaling exponents, while R_h exhibits a lower scaling exponent. Our ν estimation for the monovalent salt is around 0.76, which is consistent with that reported by Grass and Holm.³⁷ They plotted the scaling exponent as a function of the Debye length that is varied by adjusting the monovalent salt concentration and found that $\nu = 0.85$ for the salt-free solution and $\nu = 0.68$ for $c_s = 100c_{PE}$. It is noted that $c_s = c_{PE}$ is for our monovalent salt system. Scaling exponents from our simulation are $\nu = 0.75$ for the divalent salt and $\nu = 0.4$ for the trivalent salt. Wei and Hsiao reported $\nu = 0.32$ for the trivalent salt,¹⁶ which is comparable to our result. The Debye length is defined by

$$l_D = \sqrt{\frac{\epsilon_0 \epsilon_r k_B T}{2N_A e^2 I}} \quad (4)$$

where N_A is the Avogadro number and $I \propto q_s^2$ is the ionic strength of the electrolyte. With the consideration of the equivalent salt concentration, the higher valence of salt or higher ionic strength results in a smaller Debye length and thus a smaller scaling exponent. With respect to ν versus the valence of salt, our trend is monotonically decreasing, consistent with the simple theoretical analysis above: $\nu = 0.76$, 0.75, and 0.4 for the monovalent, divalent, and trivalent salt, respectively. The addition of multivalent salt into the PE solution is a simple, feasible way to collapse the PE chain. The higher valence of salt, the stronger condensation on the chain, which results in a more compact conformation of the PE chain. The results in Figure 1 are consistent with this trend of decreasing R_g , R_e , and R_h with increasing salt valence. This result is also consistent with previous simulations¹⁵ and experiments.^{38,39}

The chain end-to-end vector autocorrelation function is calculated and fit to an exponential function $\exp(-t/\tau_N)$, where τ_N gives an estimation for the longest relaxation time of the PE chain. The resulting τ_N can help us narrow down the frequency range of applied ac electric fields. Figure 2 shows the chain length dependence of τ_N for three different salts. The relaxation time is related to the time for the chain to diffuse over a distance on the order of its own size: $\tau_N \approx R^2/D$. In the Rouse model, we expect that $\tau_N \sim N^{1+2\nu}$, while the Zimm model gives $\tau_N \sim N^{3\nu}$. Our results demonstrate that the higher the salt valence, the shorter the relaxation time for the same chain length. The PE chain in the trivalent salt solution relaxes the fastest. Moreover, the scaling exponent of τ_N increases as the salt valence increases. Yet, the trend due to the Rouse model is completely the opposite. Using ν estimates from the chain conformations, we expect to obtain 2.52, 2.5, and 1.8 for the scaling exponent of the

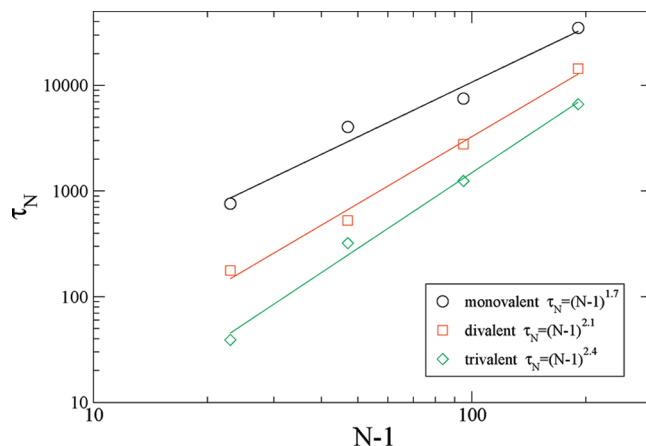


Figure 2. Chain length dependence of the longest relaxation time, τ_N , of PE chains at an equivalent concentration of different valence salt solutions.

monovalent, divalent, and trivalent salt, respectively. The discrepancy could be due to the complex behavior of PE and counterion condensation.

Chain Stretching under dc Electric Field. Next we study the chain conformation under an applied dc electric field. Previous simulations^{16,19} have shown that an external electric field can stretch the PE chain, if the field strength exceeds a critical value, E_{crit} . E_{crit} depends on the strength of electrostatic coupling, chain length, and counterion valence. By equating the polarization energy and thermal energy and using scaling arguments, Netz's approximation $E_{crit} \sim (l_B/N)^{1/2}$ gives a reasonable estimate in comparison to our simulation results.

The ratio of the end-to-end distance over the chain contour length, R_e/L , which measures the chain extension, is plotted in Figure 3 as a function of dc field strength for three different valence salt solutions. When the dc electric field is weak, R_e/L is small, indicating the chain is kept in a collapsed conformation. The increase in R_e/L with increasing field strength indicates that the PE chain becomes more extended. We also calculate the principal moments of the gyration tensor R_1^2 , R_2^2 , and R_3^2 . At small field strength $E_{dc} < E_{crit}$, the chain behaves as though there were no electric field, and the conformation is rodlike with $R_1^2 \sim N^2$ and $R_2^2 \sim R_3^2 \sim N^{1.35}$.⁹ Under strong electric fields, an increase in R_1^2 at the expense of R_2^2 and R_3^2 is observed. The dc electric field actually extends the PE conformation along the field direction (for our case the z direction) and compresses the chain perpendicular to the field direction.

The chain length dependence of critical field strength has been investigated in salt-free,¹⁹ tetravalent salt,¹⁷ and trivalent salt¹⁶ solutions. All studies showed that E_{crit} scales roughly with $N^{-1/2}$ to unfold a condensed chain. We follow Hsiao's suggestion using the inflection point in the plot of R_e/L vs E_{dc} to define E_{crit} . The obtained E_{crit} as reported in Figure 4 show that E_{crit} decreases as chain length increases for all three salts, but the rate of decrease is different, and the scaling exponent increases as the salt valence increases. Monovalent salt has the steepest drop with increasing chain length. Using multivalent salt as the condensing agent, it is easier to collapse a long PE chain but more difficult to unfold it under dc electric fields. Netz proposed that $E_{crit} \sim N^{-1/2}$ for the collapsed PE and $E_{crit} \sim N^{-3\nu/2}$ for the noncollapsed one.¹⁹ Our monovalent case belongs to the noncollapsed category and gives $E_{crit} \sim N^{-1.0}$, in good agreement with the estimated value of -1.1 by Netz. For the multivalent salt case, the exponent is smaller than Netz's estimate of -0.5 .

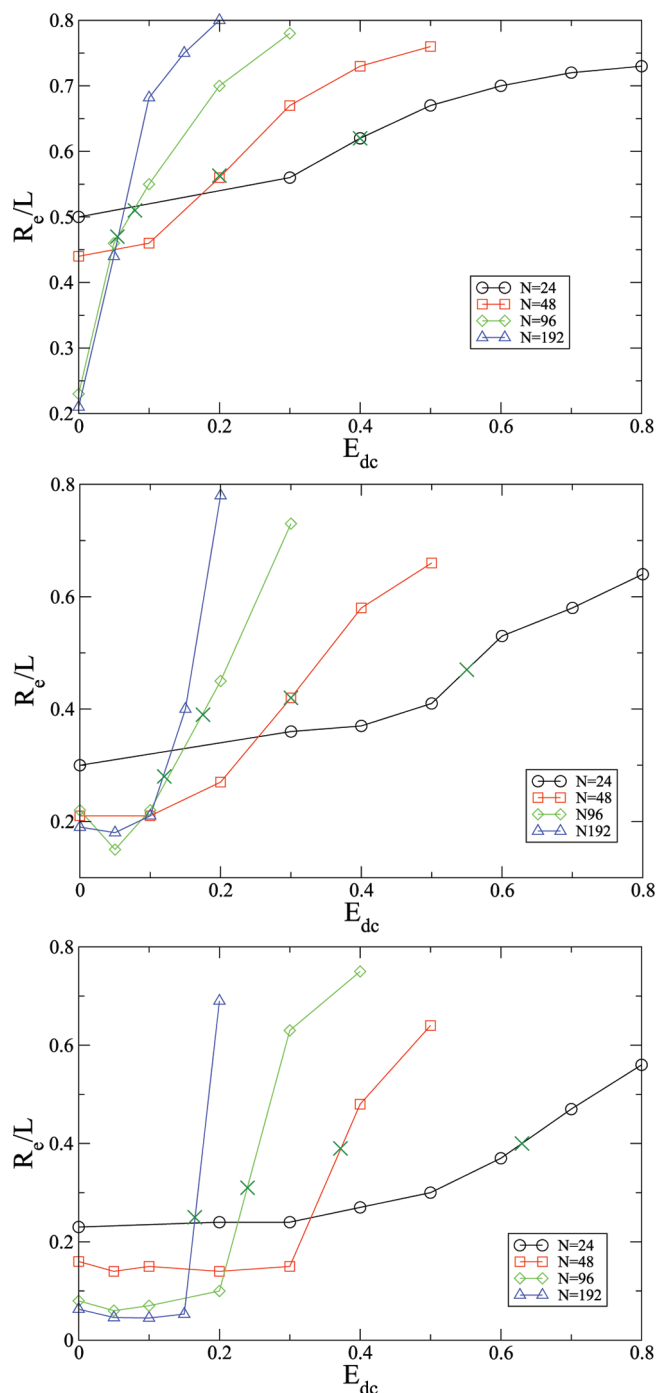


Figure 3. Field strength, E_{dc} , dependence of R_e/L at an equivalent concentration of (a) monovalent salt, (b) divalent salt, and (c) trivalent salt for various chain lengths under dc electric field. Cross symbols denote the inflection point, which determines the critical field strength.

This underestimate has also been reported by Wei and Hsiao,¹⁶ yet our exponent for the trivalent salt of -0.64 is a little bigger than their estimate of -0.77 .

Collapsed Chain Breathing and Stretching under AC Electric Field. We start with the PE of $N = 96$ in the equivalent concentration of trivalent salt to examine how a collapsed PE can be stretched under an ac electric field. A PE in the equivalent trivalent salt solution exhibits the most compact conformation. Most ac field strengths applied here are too large to keep the system in the linear response regime, so that the process is nonequilibrium. From the above sections we have shown that for our system the intrinsic frequency

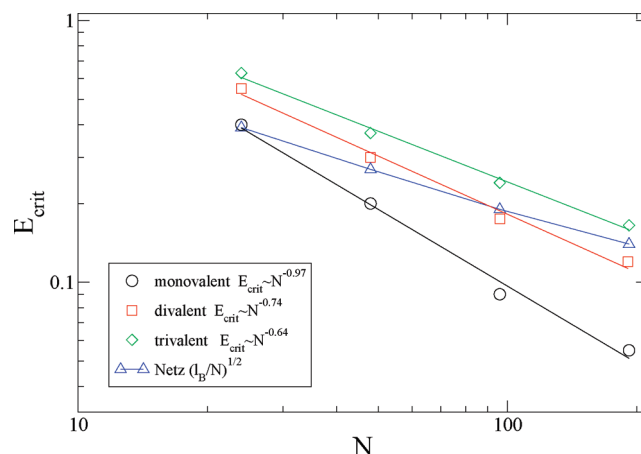


Figure 4. Chain length dependence of critical field strength, E_{crit} , at an equivalent concentration of different valent salt solutions. Theoretical estimates are included for comparison. The solid lines are power-law regression to the simulation data shown in symbols.

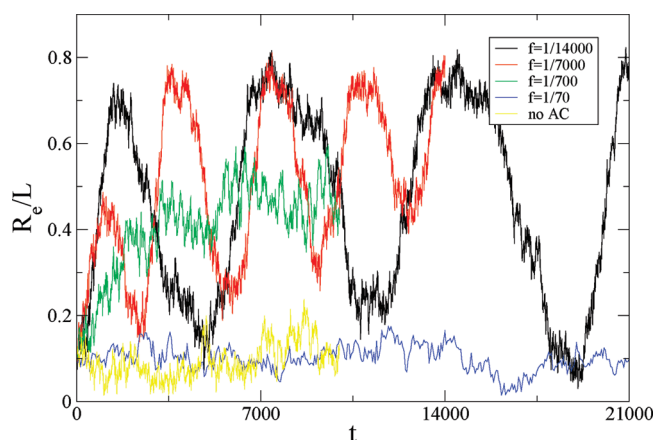


Figure 5. R_e/L evolution of a PE chain of $N = 96$ in the trivalent salt solution under an applied ac electric field at varied frequency and $E_{ac} = 0.3 > E_{crit}$. Chain conformational breathing can be observed at $f \leq 1/700$, which is comparable to $f_{intrinsic} = 1/1300$. The initial time period is a nonequilibrium process where the system responds to the applied ac field from the original collapsed state. Note that the breathing R_e/L curves have a cosine format with a period equal to one-half cycle of the ac field.

$f_{intrinsic} \sim 1/1300$ and $E_{crit} \sim 0.22$ for $N = 96$. Here we define $f_{intrinsic}$ as the inverse of the longest relaxation time, τ_N , of the chain. We first check the ac frequency dependence of chain extension by setting $E_{ac} = 0.3$. Three frequency regimes can be identified in Figure 5. First, the chain breathes and is stretched in the low-frequency regime at $f = 1/14000$ and $f = 1/7000$, where the PE and associated ions have enough time to respond to the oscillating electric field. The R_e/L curve develops three peaks and two valleys that perfectly match two positive E maxima, one negative E maximum, and two $E = 0$ points in one ac cycle. For the lowest ac frequency ($f = 1/14000$), the PE chain breathes, dynamically changing its conformation from the compact structure with $R_e/L \sim 0.1$ to the extended one where R_e is as large as 80% of its contour length. Second, the middle frequency regime at $f = 1/700$ is near the intrinsic frequency. In this regime, the PE chain also oscillates, but at a much narrower R_e/L range, which indicates that the chain does not have enough time to fully respond to the variation of the ac electric field. Third, no chain extension is observed in the high-frequency regime at $f = 1/70$. In this case, the ac frequency is so high that the PE

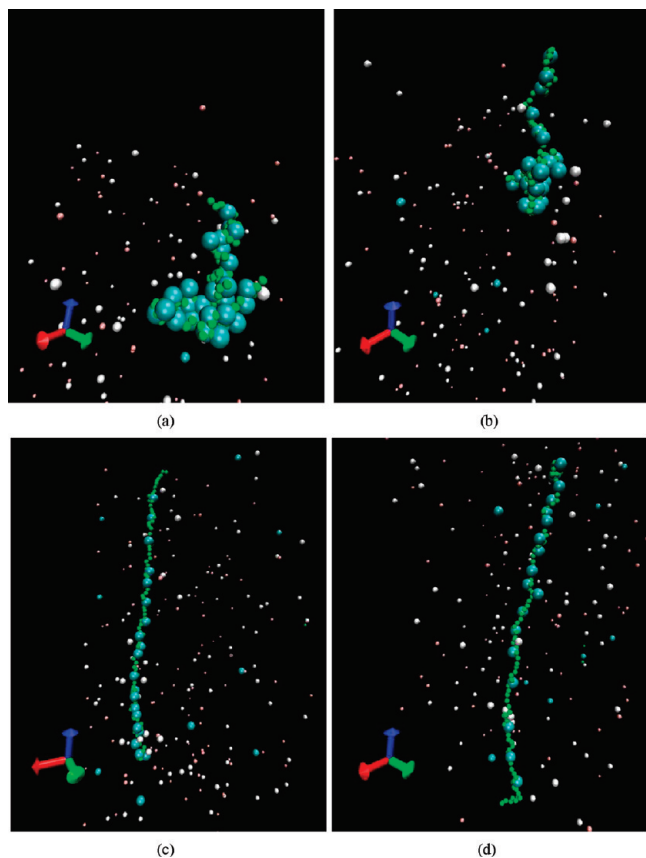


Figure 6. Representative snapshots at different phases (ϕ) of the ac cycle for $N = 96$, $f = 1/14000$, and $E_{ac} = 0.3$ at (a) $\phi = \pi/2$, showing a collapsed conformation, (b) $\phi = 4\pi/5$, showing an intermediate conformation, (c) $\phi = \pi$, showing a fully stretched state with the trivalent counterions condensed on the “down” end, and (d) $\phi = 2\pi$, showing a fully stretched state with the trivalent counterions condensed on the “up” end. The green, blue, white, and orange spheres represent monomers, trivalent counterions, monovalent counterions, and salt co-ions, respectively. Blue arrows show the z direction, along which the ac electric field is applied.

chain cannot respond to the applied electric field even though the field strength is sufficiently high. The chain conformation is thus kept similar to the one without electric fields.

Figure 6 shows some representative snapshots at different phases of the ac cycle for the chain of $N = 96$ at the applied ac field of $f = 1/14000$ and $E_{ac} = 0.3$. The ac cycle phase values of $\pi/2$, $4\pi/5$, π , and 2π correspond to instantaneous E values of 0, -0.342 , -0.423 , and 0.423 , respectively. The snapshots vividly demonstrate how the ac electric field variation affects the counterion distribution around the PE chain, which further determines the chain conformation. At a phase of $\pi/2$, $E = 0$, and the counterions are evenly distributed along the chain. It is believed that correlated charge fluctuation of counterions condensed on neighboring chain monomers generates an effective attractive force between chain monomers.⁴⁰ This attraction due to trivalent counterion condensation is strong enough to overcome the electrostatic repulsion so that the compact conformation is obtained. While at phases of π and 2π , the electric field is the strongest and counterions are driven in the field direction along the chain. The nontrivial number of trivalent counterions are actually pushed off the chain and become the free counterions. Thus, the chain becomes almost fully extended, consistent with Cohen’s theoretical prediction that a polymer extends spontaneously to its full contour length at a

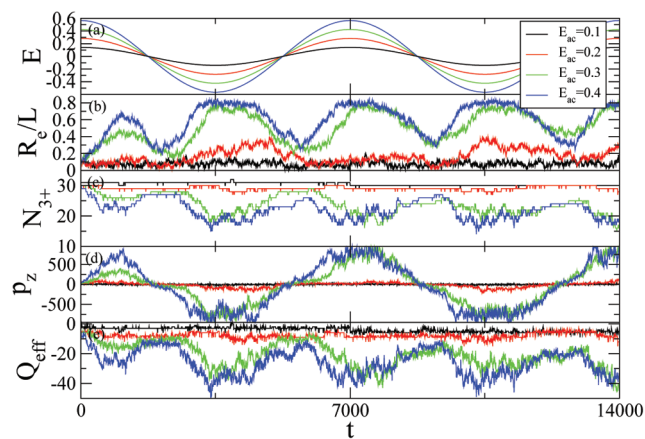


Figure 7. A PE chain of $N = 96$ in the equivalent trivalent salt solution under an ac field of $f = 1/7000 < f_{intrinsic} = 1/1300$ and varied E_{ac} . (a) Two ac cosine-wave electric cycles. Note that the peak field strength value of the ac field is $2^{1/2}E_{ac}$. (b) The chain extension R_e/L , the stretching and breathing can be observed only at $E_{ac} > E_{crit} = 0.22$. (c) The number of condensed trivalent counterions N_{3+} . For the breathing cases, N_{3+} shows the periodic behavior with a frequency of $2f$. At the vanishing field, N_{3+} reaches the maximum while at the strongest field, it reaches the minimum. (d) The dipole moment of the PE-ion complex along the electric field z direction p_z . It demonstrates that the periodic behavior of p_z is similar to the E oscillation for all field strengths studied in this work. p_z solely arises from the induced migration of counterions by the applied electric field. (e) The effective charge associated with the PE chain, Q_{eff} . The pattern follows that of N_{3+} in panel c.

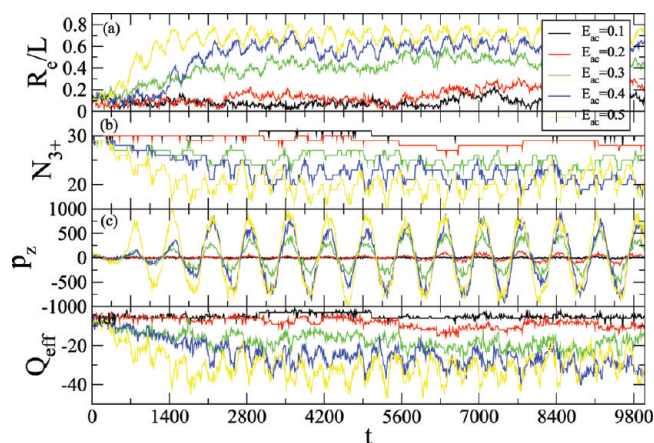


Figure 8. A PE chain of $N = 96$ in response to the ac electric field of $f = 1/700$ at varied E_{ac} in the equivalent trivalent salt solution in terms of (a) the chain extension, R_e/L , (b) the number of the condensed trivalent counterions, N_{3+} , (c) the dipole moment of PE-ion complex along the field direction, p_z , and (d) the effective charge, Q_{eff} , associated with the PE chain.

sufficiently strong ac field.³⁰ At phase of $4\pi/5$, the chain shows the intermediate conformation between the compact and extended.

Figure 7 shows the PE of $N = 96$ in response to an ac field of $f = 1/7000$ in the trivalent salt solution. The corresponding ac electric field is presented in Figure 7a. The field strength has to exceed a certain threshold value to observe the chain breathing. The stronger the field strength, the longer the chain stays in the elongated conformation. The threshold ac field strength is consistent with the critical value ($E_{crit} = 0.22$) found in the dc-field simulation. At $E_{ac} > E_{crit}$, the chain can breathe with R_e/L oscillating at a range of 0.3 – 0.8 . When the field strength is around E_{crit} , the chain responds to the

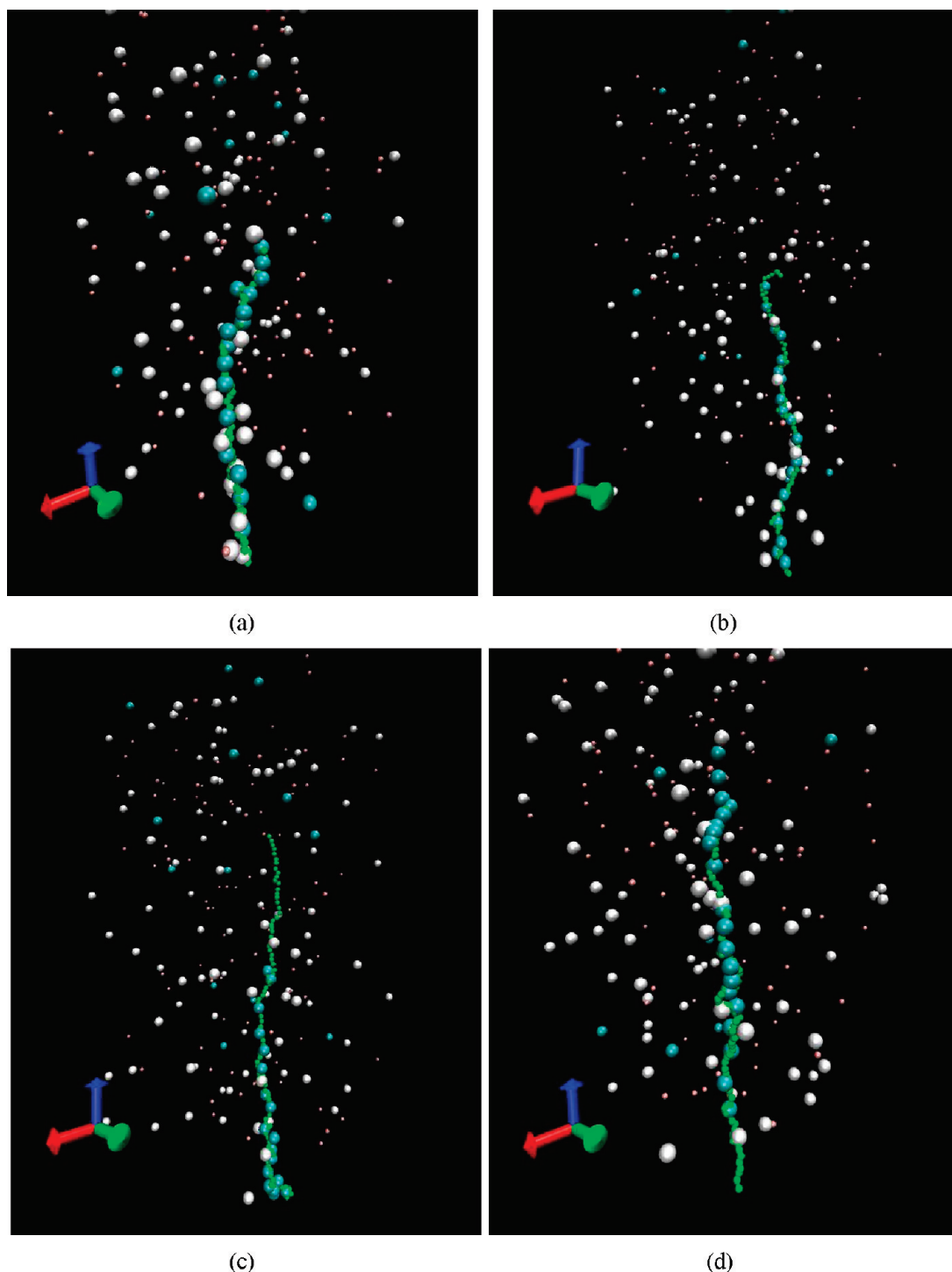


Figure 9. Representative snapshots at different phases (ϕ) of the ac cycle for $N = 96$, $f = 1/700$, and $E_{ac} = 0.5$. (a) $\phi = \pi/2$; (b) $\phi = 4\pi/5$; (c) $\phi = \pi$; (d) $\phi = 2\pi$. The green, blue, white, and orange spheres represent monomers, trivalent counterions, monovalent counterions, and salt co-ions, respectively. Blue arrows show the z direction, along which the ac electric field is applied.

electric field, but R_c/L peak–valley oscillating pattern does not develop very well. At $E_{ac} < E_{crit}$, no chain breathing or stretching is observed. The dipole moment of the PE–ion complex induced by the electric field is calculated by $p = \sum_i q_i (\vec{r}_i - \vec{r}_{com})$, where \vec{r}_{com} is the center of mass of the PE. We assume that the ions within a distance of 2.5 to the PE chain belong to the complex and are considered as the condensed ions. The condensed trivalent counterion evolution is shown in Figure 7c. At $E_{ac} > E_{crit}$, a clear peak–valley structure for counterions is observed. When the field strength is small, it is easier for trivalent counterions to

condense on the chain than for monovalent ones: N_{3+} reaches a maximum, while N_{1+} is at a minimum. At the strongest field, no matter which direction the field is in either $+z$ or $-z$, trivalent counterions are more easily to be stripped off from the chain than monovalent counterions: N_{3+} reaches a minimum, while N_{1+} is at a maximum. The dipole moment of the complex along the field direction is shown in Figure 7d. p_z shows the periodic behavior similar to the oscillatory ac field over the entire field strength range. Even at $E_{ac} = 0.1$, we do not see chain breathing and stretching in the R_c/L evolution curve, yet we do observe that p_z responds

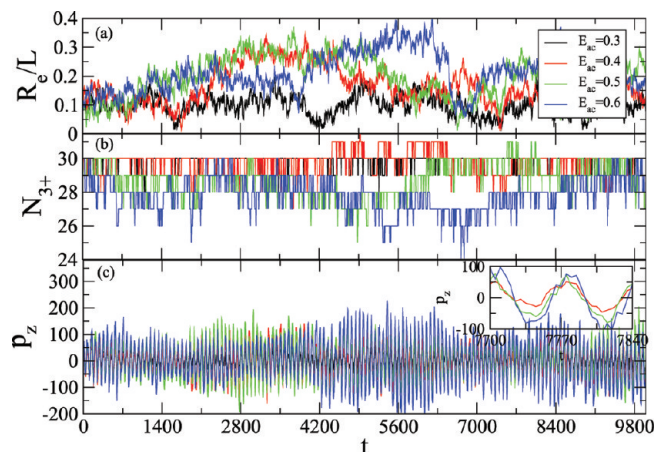


Figure 10. A PE of $N = 96$ in response to the high-frequency ac electric field of $f = 1/70$ at varied E_{ac} in the equivalent trivalent salt solution, in terms of (a) the chain extension R_e/L . No substantial stretching is observed even for $E_{ac} = 0.6$. Also, no breathing is seen; (b) the number of the condensed trivalent counterions N_{3+} , (c) the dipole moment p_z of PE-ion complex along the field direction. p_z shows a periodic behavior similar to the applied electric field. The inset shows the time period over two ac cycles. The response of p_z show a slight lag behind the variation of the ac electric field.

to the ac oscillation. Such a response can only be observed along the field direction, yet not at the other two directions. Our results suggest that the oscillation in p_z is necessary but not sufficient to induce the chain breathing. We also calculate the induced dipole moment of the chain and find that it is negligible in all three directions, supporting the widely accepted view in the literature that the stretching of biological PEs is mainly due to the counterion polarization. The integrated effective charge Q_{eff} , which denotes the total charge inside a wormlike tube with the chain as the center, behaves similar to N_{3+} shown in Figure 7e, which implies trivalent counterions are a dominant factor in the counterion condensation process.

Figure 8 shows how R_e/L depends on the field strength at a moderate frequency of $f = 1/700$. Again, we note that the field strength has to exceed E_{crit} to observe the chain breathing and stretching phenomena. When the field strength is less than E_{crit} , for instance at $E_{ac} = 0.1$ and 0.2 , R_e/L fluctuates around 0.1 and 0.2 , respectively. At large field strengths, the chain breathes with the applied ac field. The larger the field strength, the faster R_e/L reaches a steady state and the greater the value of R_e/L . The condensed trivalent counterions, dipole moment of the PE-ion complex, and effective charge are shown in parts b, c, and d of Figure 8, respectively. p_z shows the periodic oscillation for all field strength values since all field strengths exceed the limit of the linear response. N_{3+} and Q_{eff} exhibit periodic behavior only at $E_{ac} > E_{crit}$. Several representative snapshots of the PE system at $f = 1/700$ are shown in Figure 9. The major difference between these results and those shown in Figure 6 is that for the vanishing instantaneous E at phase of $\pi/2$ the chain cannot get back the original compact conformation; instead, it is kept in an elongated conformation with a moderate extension.

In Figure 10, the response of a PE chain of $N = 96$ under a high-frequency ac electric field of $f = 1/70$ with varied field strength is shown. At this frequency, the ac field can do nothing but shift R_e/L to slightly higher values with increasing field strength. The periodic oscillation of p_z is observed. The higher E , the bigger the magnitude of oscillation. No periodic behavior is seen in N_{3+} . The similar behavior is

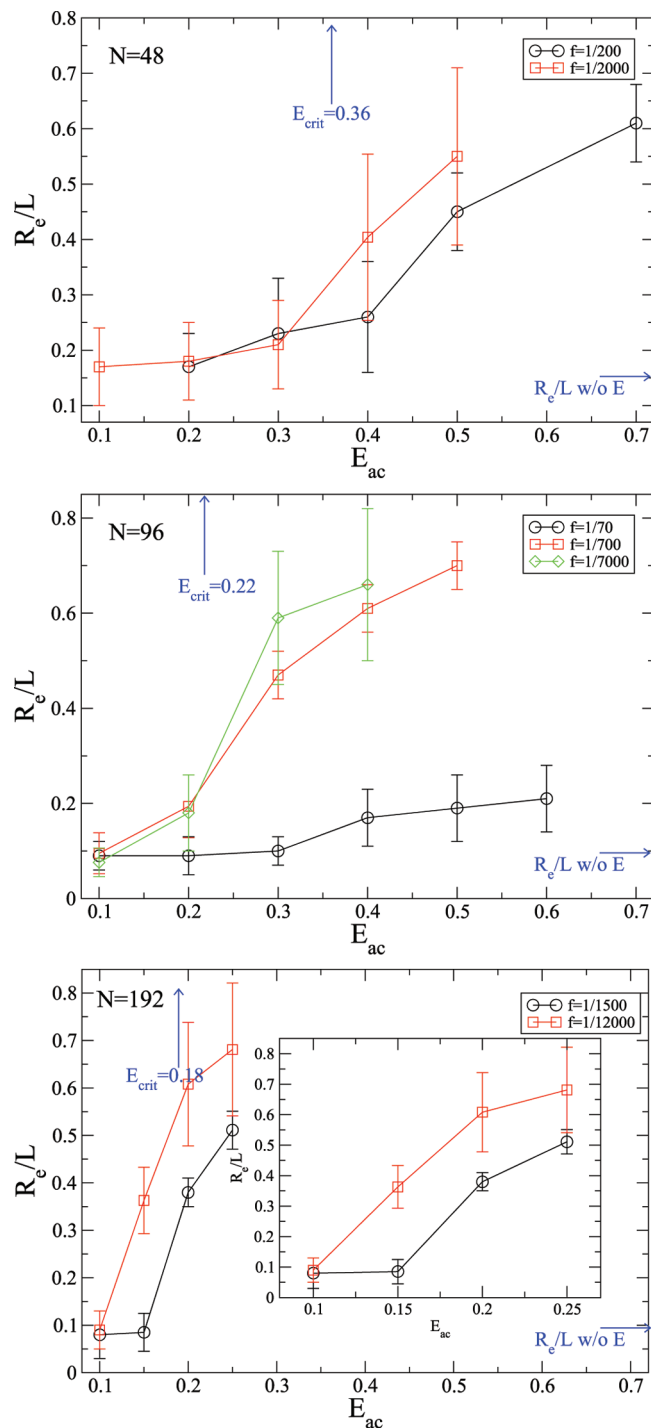


Figure 11. Field strength, E_{ac} , dependence of the average R_e/L at different ac frequencies at the equivalent trivalent salt for PE chains of different chain length of (a) $N = 48$, (b) $N = 96$, and (c) $N = 192$. The inset is a closeup for (c). R_e/L values in the absence of an electric field and critical field strengths under an dc field are indicated by arrows. Note that the conformational transition becomes sharper with increasing chain length.

observed for other chain lengths of $N = 48$ and $N = 192$ (results not shown), thus conforming the generality of ac-induced conformational stretching.

The PE chain stretching under an ac field is quantified by averaging the R_e/L oscillation at steady state. The range of R_e/L determines the average and deviation. The average R_e/L as a function of field strength is shown in Figure 11 for $N = 48, 96$, and 192 . Substantial stretching can only be

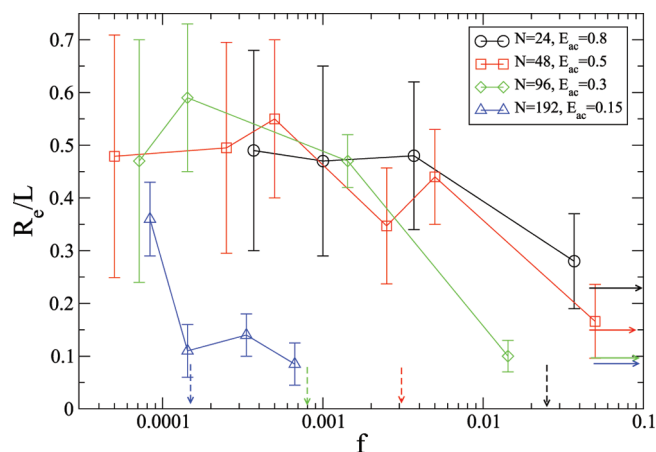


Figure 12. The ac frequency dependence of average R_e/L at different chain lengths at the equivalent trivalent salt. E_{ac} is set to be greater than the corresponding E_{crit} . The solid arrows denote R_e/L values without electric field. The dash arrows indicate the corresponding intrinsic frequencies.

obtained at applied field strength greater than the corresponding E_{crit} . Below E_{crit} , the PE chain keeps the conformation approximate to that without the electric field. It should be noted that frequencies used here are less than or comparable to the intrinsic frequencies, except at $f = 1/70$ as shown in Figure 11b. As $f = 1/70$ is much larger than $f_{intrinsic} = 1/1300$, no stretching is observed even at $E_{ac} = 0.6$. The ac frequency dependence of average chain extension at varied E_{ac} is shown in Figure 12. This plot emphasizes the importance of the ac frequency to stretch the PE chain. All E_{ac} applied are strong enough to exceed the respective E_{crit} . To stretch the chain, the applied ac frequency must be less than or comparable to the intrinsic frequency of the chain. To summarize, these two requirements (the critical ac field strength and frequency) must be satisfied simultaneously in order to stretch the PE chain under an applied ac field. It is also important to compare our findings to experimental data. Dukkupati and Pang²⁵ stretched λ -DNA in a microchannel using high-frequency ac fields and found that on increasing frequency from 100 kHz to 1 MHz, the chain conformation undergoes a transition from fully stretched to no stretching. This trend is consistent with our simulation for all chain lengths. They found that the DNA stretched length decreases as the ac field strength is decreased, which also agrees well with our data as shown in Figure 11. Another relevant work⁴¹ by the Walti group showed that DNA stretching first increases and then decreases with increasing frequency. Full extension of the DNA chain is found at frequencies of 200–300 kHz, and this maximum is independent of the chain length. Instead, our simulations show the chain extension increases as frequency decreases, yet we do not observe the reduction in chain extension in the low-frequency regime. Moreover, our stretching frequency shows a strong chain length dependence. The discrepancy between simulation and experiments at low frequencies may be due to the fact the effective field is reduced owing to the electrode polarization in the ac experiments, leading to a substantial decrease in the dipole moment and the dielectrophoretic torque.^{41,42}

Noncollapsed Chain Breathing and Stretching under AC Electric Field. In this section, we study the behavior of a noncollapsed PE in a monovalent salt system. We first investigate the ac frequency dependence of the chain conformation shown in Figure 13. To facilitate the comparison

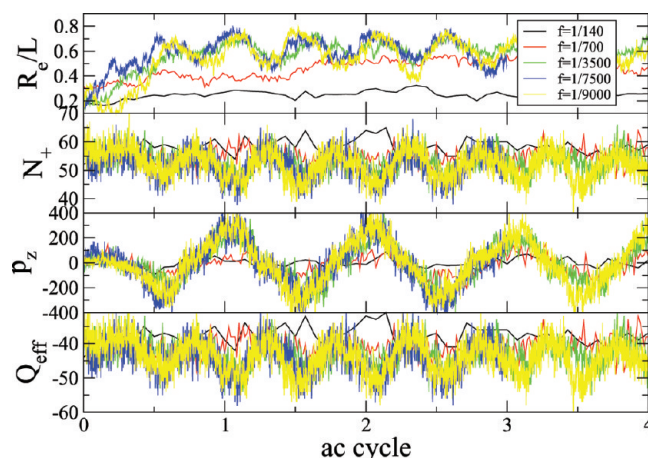


Figure 13. A PE chain of $N = 96$ in response to the ac electric field at varied f and $E_{ac} = 0.15 > E_{crit}$ in the equivalent monovalent salt solution. The x axis is the product of time and frequency, equivalent to the ac cycle. (a) The chain extension R_e/L . When ac frequency is comparable to or smaller than $f_{intrinsic} = 1/7500$, breathing and stretching are observed. (b) The number of the condensed counterions N_+ . Counterions and salt counterions are indistinguishable. (c) The dipole moment p_z of PE-ion complex along the field direction. (d) The effective charge Q_{eff} associated with the PE chain.

between different frequencies, the time axis normalized by frequency is transformed to the number of ac cycles. The field strength of $E_{ac} = 0.15$ is set to be greater than the respective E_{crit} . We observe a clear breathing process when the applied ac frequency is less than or equal to $f_{intrinsic} = 1/7500$, with R_e/L oscillating between 0.5 and 0.8. The dipole moment of the complex follows the variation of the applied ac electric field. The number of condensed monovalent counterions including counterions and salt counterions also shows a periodic evolution. Additionally, the integrated effective charge of the PE chain demonstrates that the periodic behavior is intimately associated with the applied ac field.

At the high frequencies of $f = 1/140$ and $1/700$, the chain behaves differently from the collapsed chain case. High ac frequency field extends the PE chain, with R_e/L values approaching the one observed in the dc field. The similarity suggests that the ac response is similar to the dc response at the high-frequency regime for the monovalent salt system. The dipole moment of the complex, associated ions, and effective charge show no periodic behavior either. The dipole moment at $f = 1/700$ shows a weak periodic behavior, but that does not necessarily lead to the breathing phenomena. The induced dipole moment still has to be strong enough to overcome thermal fluctuation in order to induce chain breathing.

The ac frequency dependence of chain extension at $E_{ac} = 0.08$, which is around the critical value is also studied (results not shown). At low frequencies of $f = 1/3500$, $1/7500$, $1/10000$, and $1/15000$, the dipole moment of the complex shows a periodic behavior, yet R_e/L displays no breathing. Over the entire frequency range of $f = 1/7 - 1/15000$, the ac field acts on a PE chain in a similar manner as the dc field does. The PE chain extends to almost one-half of its contour length.

Discussion. Our molecular dynamics simulations have demonstrated that the PE chains exhibit a breathing response to the ac electric field only when the ac field strength exceeds a critical value and the ac frequency is comparable to or less than the intrinsic frequency of a PE chain. Our results also suggest the valency of condensing agents has a strong effect on the PE behavior under the ac electric field. With added

multivalent salt, the PE response is consistent with experimental observation. At high frequency, the chain keeps the original conformation because the chain does not have enough time to respond to the fast variation of the electric field; when the frequency is low enough, the PE resonates with the oscillating field, resulting in a “breathing” behavior where the chain alternately collapses and stretches. In contrast, with added monovalent salt, the chain always responds to the field, even at very high frequency such as at $f = 1/7$. The predicted trend for the monovalent salt is that with decreasing ac frequency the PE chain undergoes a transition from a dc field like response to a breathing behavior. In future work, it would be worth studying the effect of salt concentration, chain stiffness, and PE concentration on the conformational dynamics of the PE chain. Also, simulation with hydrodynamic interaction deserves further study.

IV. Conclusion

We have studied the behavior of a flexible PE chain with explicit salt by means of a coarse-grained molecular dynamics simulation. In the absence of an electric field, we have found the scaling exponent $\nu = 0.76, 0.75$, and 0.4 for an equivalent solution of the monovalent, divalent, and trivalent salt, respectively. We have also predicted the power law dependence of the longest relaxation time of the PE chain with the exponent of $1.7, 2.1$, and 2.4 for monovalent, divalent, and trivalent salt. Under a dc electric field, the chain is unfolded when the field strength is larger than a critical value. The critical field strength shows a power law against chain length, and the corresponding exponents are $-0.97, -0.74$, and -0.64 for monovalent, divalent, and trivalent salt, respectively. The critical field strength obtained from the dc field simulation is also used to set the critical field strength in the ac field simulation. The conformational response of a PE chain to an ac field is reported with the dependence of ac frequency, field strength, and salt valence. Our results under applied ac fields show that the chain can breathe and become stretched only when the field strength exceeds the critical field strength, and the ac frequency is comparable to or less than the intrinsic frequency of the chain, which is the reciprocal of the longest chain relaxation time. Trivalent salt has a much stronger effect on the conformational structure of PEs than monovalent salt. It is also confirmed that ac electric field can effectively modify the counterion distribution near the PE chain, which is critical to control the PE chain conformation.

Acknowledgment. The authors acknowledge the Northwest Indiana Computational Grid (NWICG) for funding this research. Y.Z. also acknowledges the financial support by the U.S. Department of Energy, Office of Basic Energy Sciences, Materials Sciences and Engineering Division (DE-FG02-07ER46390). The authors thank Craig Tenney for adding the ac field capability to the LAMMPS package. The Center for Research Computing at the University of Notre Dame is gratefully acknowledged for computational resources.

References and Notes

- (1) Dolnik, V. *Electrophoresis* **2006**, *27*, 126–141.
- (2) Cottet, H.; Simões, C.; Vayaboury, W.; Cifuentes, A. *J. Chromatogr. A* **2005**, *1068*, 59–73.
- (3) Muthukumar, M. *Electrophoresis* **1996**, *17*, 1167–1172.
- (4) Grass, K.; Böhme, U.; Scheler, U.; Cottet, H.; Holm, C. *Phys. Rev. Lett.* **2008**, *100*, 096104.
- (5) Frank, S.; Winkler, R. G. *Europhys. Lett.* **2008**, *83*, 38004.
- (6) Grass, K.; Holm, C. *Faraday Discuss.* **2010**, *144*, 57–70.
- (7) Long, D.; Ajdari, A. *Eur. Phys. J. E* **2001**, *4*, 29–32.
- (8) Tanaka, M.; Grosberg, A. Y. *J. Chem. Phys.* **2001**, *115*, 567–574.
- (9) Stevens, M. J.; Kremer, K. *J. Chem. Phys.* **1995**, *103*, 1669–1690.
- (10) Liu, S.; Ghosh, K.; Muthukumar, M. *J. Chem. Phys.* **2003**, *119*, 1813–1823.
- (11) Deserno, M.; Jiménez-Ángeles, F.; Holm, C.; Lozada-Cassou, M. *J. Phys. Chem. B* **2001**, *105*, 10983–10991.
- (12) Stevens, M.; Plimpton, S. *Eur. Phys. J. B* **1998**, *2*, 341–345.
- (13) Wei, Y.-F.; Hsiao, P.-Y. *J. Chem. Phys.* **2007**, *127*, 064901.
- (14) Hsiao, P.-Y.; Luijten, E. *Phys. Rev. Lett.* **2006**, *97*, 148301.
- (15) Liu, S.; Muthukumar, M. *J. Chem. Phys.* **2002**, *116*, 9975–9982.
- (16) Wei, Y.-F.; Hsiao, P.-Y. *Biomechanics* **2009**, *3*, 022410.
- (17) Hsiao, P.-Y.; Wu, K.-M. *J. Phys. Chem. B* **2008**, *112*, 13177–13180.
- (18) Ueda, K.; Izumi, N.; Sakomura, M. *Bull. Chem. Soc. Jpn.* **2005**, *78*, 430–434.
- (19) Netz, R. R. *J. Phys. Chem. B* **2003**, *107*, 8208–8217.
- (20) Netz, R. R. *Phys. Rev. Lett.* **2003**, *90*, 128104.
- (21) Elvingson, C. *Biophys. Chem.* **1992**, *43*, 9–19.
- (22) Suzuki, S.; Yamanashi, T.; Tazawa, S.; Kurosawa, O.; Washizu, M. *IEEE Trans. Ind. Appl.* **1998**, *34*, 75–83.
- (23) Asbury, C. L.; van den Engh, G. *Biophys. J.* **1998**, *74*, 1024–1030.
- (24) Asbury, C. L.; Diercks, A. H.; van den Engh, G. *Electrophoresis* **2002**, *23*, 2658–2666.
- (25) Dukkupati, V. R.; Pang, S. W. *Appl. Phys. Lett.* **2007**, *90*, 083901.
- (26) Kim, J. H.; Dukkupati, V. R.; Pang, S. W.; Larson, R. G. *Nanoscale Res. Lett.* **2007**, *2*, 185–201.
- (27) Hölzel, R. *IET Nanobiotechnol.* **2009**, *3*, 28–45.
- (28) Washizu, H.; Kikuchi, K. *J. Phys. Chem. B* **2002**, *106*, 11329–11342.
- (29) Wälti, C.; Tosch, P.; Davies, A. G.; Germishuizen, W. A.; Kaminski, C. F. *Appl. Phys. Lett.* **2006**, *88*, 153901.
- (30) Cohen, A. E. *Phys. Rev. Lett.* **2003**, *91*, 235506.
- (31) Ueda, M.; Oana, H.; Baba, Y.; Doi, M.; Yoshikawa, K. *Biophys. Chem.* **1998**, *71*, 113–123.
- (32) Ueda, M. *J. Biochem. Biophys. Methods* **1999**, *41*, 153–165.
- (33) Kaji, N.; Ueda, M.; Baba, Y. *Appl. Phys. Lett.* **2003**, *83*, 3413–3415.
- (34) Kaji, N.; Ueda, M.; Baba, Y. *Biophys. J.* **2002**, *82*, 335–344.
- (35) Plimpton, S. *J. Comput. Phys.* **1995**, *117*, 1–19.
- (36) Weeks, J. D.; Chandler, D.; Andersen, H. C. *J. Chem. Phys.* **1971**, *54*, 5237–5247.
- (37) Grass, K.; Holm, C. *Soft Matter* **2009**, *5*, 2079–2092.
- (38) Zhang, Y.; Douglas, J. F.; Ermi, B. D.; Amis, E. J. *J. Chem. Phys.* **2001**, *114*, 3299–3313.
- (39) Prabhu, V. M.; Muthukumar, M.; Wignall, G. D.; Melnichenko, Y. B. *Polymer* **2001**, *42*, 8935–8946.
- (40) Winkler, R. G.; Gold, M.; Reineker, P. *Phys. Rev. Lett.* **1998**, *80*, 3731–3734.
- (41) Germishuizen, W. A.; Tosch, P.; Middelberg, A. P. J.; Wälti, C.; Davies, A. G.; Wirtz, R.; Pepper, M. *J. Appl. Phys.* **2005**, *97*, 014702.
- (42) Ramos, A.; Morgan, H.; Green, N. G.; Castellanos, A. *J. Phys. D* **1998**, *31*, 2338–2353.